TESTING A ROBOTIC SYSTEM FOR COLLECTING AND TRANSFERRING SAMPLES ON MARS

Tony Jorden [(1)], Elie Allouis [(1)], Nildeep Patel [(1)], Joe Smith [(1)] , Tobias Welge-Lüssen [(2),], Rudolf Spörri [(2)] , Samuel Senese [(3),], Rolando Gelmi[(3),],Konstantinos Kapellos [(4)] , Roger Pissard-Gibollet[(4)] , Roberto Ferrario [(5)] Gianfranco Visentin [(6)]

[(1)] Astrium Ltd, Gunnels Wood Road, Stevenage, SG1 2AS, UK, tony.jorden@astrium.eads.net
[(2)] Ruag Space, Schaffhauseerstrasse 580, CH-8052 Zurich, Switzerland,: rudolf.spoerri@ruag.com
[(3)] Selex-Galileo, Viale Europa, 20014, Nerviano (MI), Italy, samuel.senese@selexgalileo.com
[(4)] Trasys SA, Rozendal Park, Terhulpsesteenweg 6c, 1560 Hoelaart, Belgiim, Konstantinos.Kapellos@trasys.be
[(5)] Tecnomare S.p.A., Via Pacinotti 4, 30175 Ve Marghera, Italy, Roberto.Ferrario@tecnomare.it
[(6)] ESA– ESTEC, Keplerlaan 1 Postbus 299, NL2200 AG Noordwijk,The Netherlands, gianfranco.visentin@esa.int

ABSTRACT

Handling samples of material on planetary surfaces, requires a complex autonomous robotic chain for a sample-return mission. From the ESA-funded Mars Surface Sample Transfer and Manipulation Study, the research described here is particularly targeting a potential Mars Sample Return (MSR) mission -proposed for mid 2020s. Based on a preliminary design of the end-to-end sample-handling chain, critical elements were selected for breadboard tests. One breadboard was built to collect and package soil samples in sample vessels. Secondly, an end-effector for a robotic arm was built. The third breadboard was a detailed software simulation of the overall transfer chain, supplemented by some vision-control hardware tests. Testing verified critical aspects of the performance and validated the designs of these key elements of the robotics chain. This paper presents the designs and the latest results from the test campaign.

1. INTRODUCTION

Figure 1 illustrates the top-level elements for collecting samples on the surface of Mars and especially the 'mobile' scenario where samples are collected by a rover which then takes the samples to an ascent vehicle for return to Earth.

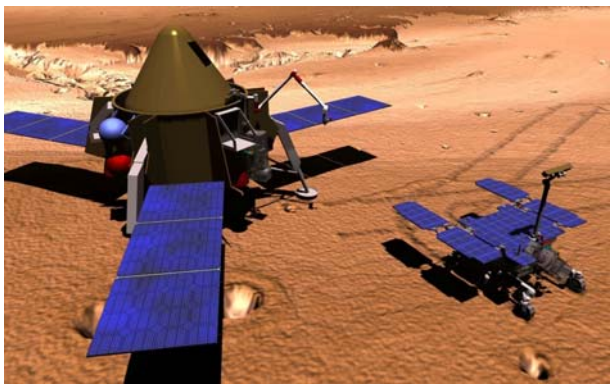

Figure 1- Overview of a sample collection mission

The return of a sample from Mars will allow detailed scientific analysis to help answer questions about the nature of Mars, its formation, and the possibility of life on another planet. Various mission architectures are under consideration, and are evolving. For example, it is likely that a rover will do the sample collection. In an alternative mission architecture, samples would be collected only at the lander. However, all such missions have a common fundamental requirement - to collect a sample on the surface and transfer it to a vehicle for return to Earth. The sub-systems (Figure 2) required for sample-handling are similar whatever the architecture.

A detailed study of concepts, leading to a preliminary design of the end-to-end Surface Sample-Handling System (SSHS), has been carried out and reported previously [1]. This led to the selection of critical elements for breadboard (BB) tests:

(a) Sample capping and uncapping mechanism (to secure a soil sample in an individual sample vessel, within an overall sample container). The tests assess the performance of the automated mechanism, including performance in the presence of dust, and sample collection from a drill.

(b) End-effector (EE). This device is required to securely grasp a sample container and to tighten a bolt that holds sample container halves together. The tests examine self-alignment capability (end-effector with respect to the sample container), as well as the performance of the locking and tightening of the securing screw. Thermal effects and the effects of dust have also been examined.

(c) Vision control of a robotic arm (for sample transfers to a Mars ascent vehicle), together with detailed simulation of robotic arm control. This later simulation is used to examine in detail all the aspects of using a robotic arm to pick up a sample container (from a Mars rover or a lander-based drill), transfer it to an ascent vehicle, and secure it in the ascent vehicle.

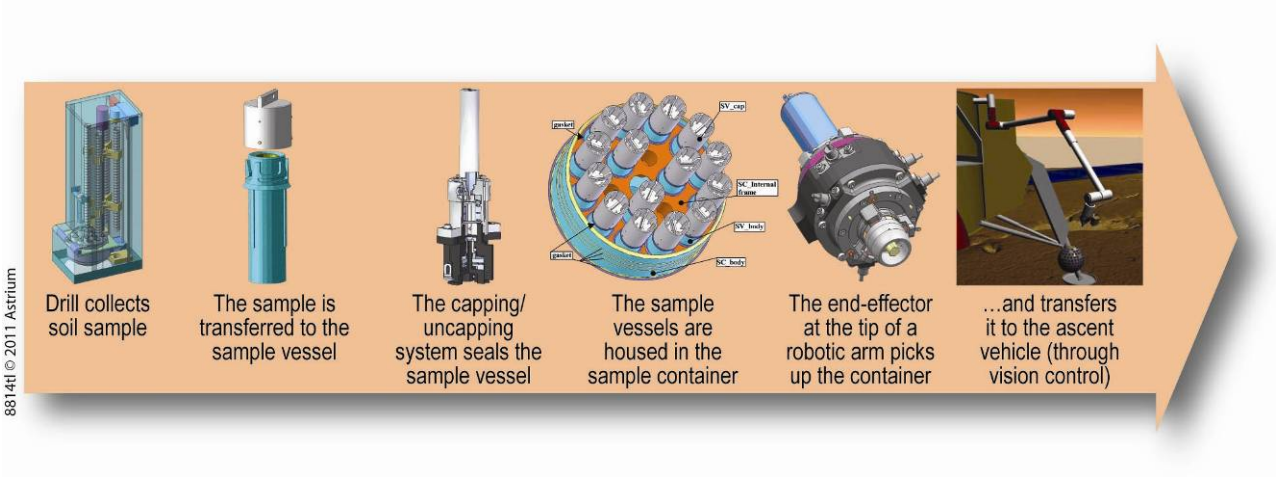

Figure 2- Main elements of the robotic sample handling chain

As Figure 2 illustrates, the breadboards that were tested represent the main elements of the sample handling, excluding the drill that has been studied previously [2].

2. SAMPLE PACKAGING

2.1. Design

Several elements were designed and assembled into one overall bread-board test assembly, as shown below.

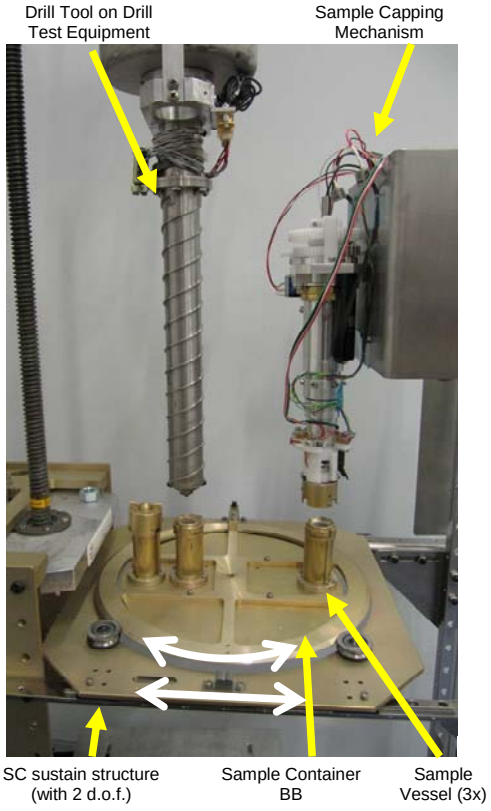

Figure 3- Sample packaging test assembly

Figure 3 shows the main components of the test assembly, which was used to assess the performance of sub-systems associated with the sample packaging:

- Sample Vessel (SV) breadboard
- Sample Container (SC) interface breadboard-
- Sample Capping & Uncapping Mechanism (SCM).
- They were all assembled and attached to a Drill Test Equipment already available at Selex Galileo.
- The SC support structure has 2 Degrees of Freedom (DOF), with self-alignment capabilities. This unit allowed the Sample Vessel to be positioned under the SCM and the Drill Tool.

Figure 4 shows a detailed view of the SCM. The 3-DOF system is able to translate, rotate and clamp the SV cap.

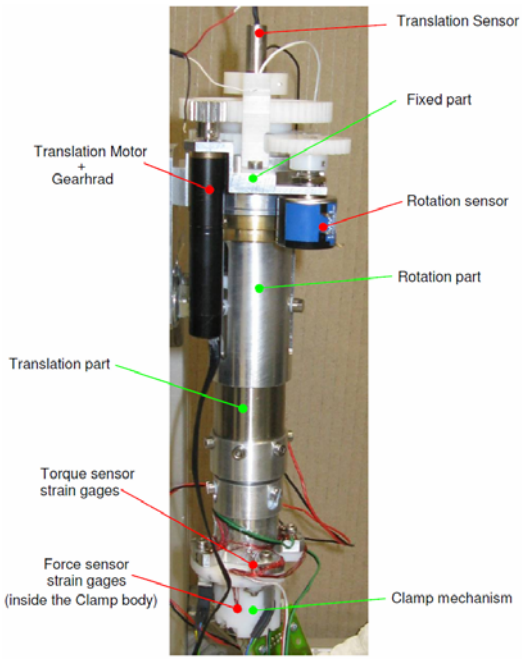

Figure 4- Breadboard of the capping mechanism

The SV BB (shown in Figure 5) was similar to the version conceived for the Mars Sample Return mission, with the exception of the gasket (which is made of lead instead of gold) and the inner diameter (here adjusted for BB purposes to a 14mm dia. sample instead of the 20mm dia. sample foreseen in the flight version).

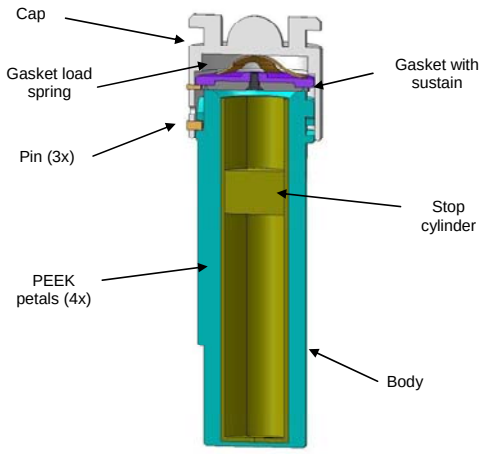

Figure 5 - Breadboard of the sample vessel

2.2. Test Aims

With these hardware devices, and a custom designed software control system, a test campaign was performed to asses the actual capabilities of the Sample Handling System on the following aspects:

- Uncapping of the sample vessel
- Sample Discharge from Drill Tool into the SV.
- Capping of the sample vessel
- Sample Extraction from the sample vessel
- Self alignment of the Sample Container (rotation & translation degrees-of-freedom)
- Preservation of sample stratigraphy - during sample discharge
- Sealing of the sample vessel.

2.3. Test Results

For each of the first three aspects more than 30 single operations were successfully performed, each time recording the main parameters characterizing the interactions between the various acting devices (among which the thrust and torque levels). Figure 6 illustrates the key steps followed during a Sample Vessel uncapping operation.

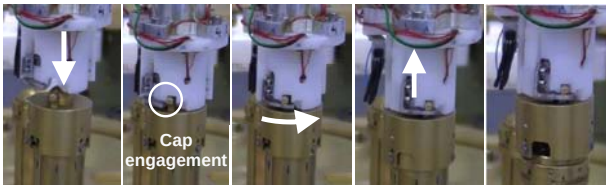

Figure 6 - Steps of the uncapping operation sequence

The extraction of the sample from the SV (an operation to be performed once on Earth) was investigated with an additional, dedicated test setup, shown in Figure 7. Here the SV base was equipped with four dead holes closed by a thin metallic layer. The idea is to punch them with a piston ("pusher" in Figure 7) and break open the four holes.

The test setup allowed investigation of different layer thicknesses (0.05 mm, 0.10 mm, and 0.15 mm), and allowed the pin design to be refined, from a flat-head design to a V-shaped design. This modification allowed the required force to be reduced to 38% of the original one, reaching 380N only for a 0.05mm thin layer.

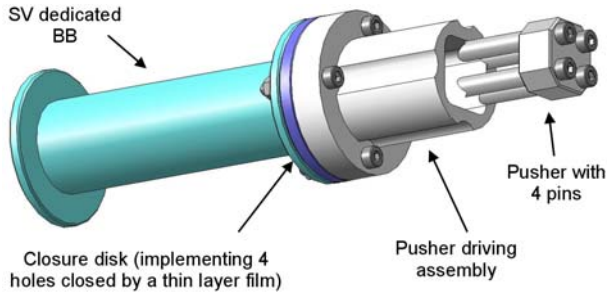

Figure 7- Setup for the Sample extraction test

The test of the self-alignment capabilities of the Sample Container support structure was based on the same sequence of actions foreseen for the uncapping, sample discharge and capping operations. However, before each operation, a misalignment was imposed to the Sample Container referred to either the Sample Capping Mechanism or the Drill Tool.

The test has been performed many times, and demonstrated a good alignment capability for each of the three mechanical interfaces. They exceed the values indicated during the design for each interface:

- SCM / SV cap: 6mm / 2°
- SV cap / SV body: 3mm / 1°
- Drill Tool / SV body: 3mm / 8°

Sample discharge was also performed with both solid and unconsolidated samples to investigate the capability to preserve the stratigraphy of the collected sample. For this purpose, a stop cylinder was included into the sample vessel body to avoid the sample abruptly falling from the Drill Tool (a piston/shutter based device) into the Sample Vessel.

For the solid sample the performance was as designed, and the stratigraphy was preserved. For the unconsolidated sample, the not-optimized interface between the SV and the Drill Tool (inherited from a previous project and not designed for compatibility with any SV) led some material accumulating near the SV rim and spilling into the SC base-plate, as a result of the clearance between SV body and Drill Tool.

Tests were however performed with various control conditions. Thus, it was seen that avoiding the rotation

of the Drill Tool during the discharge could be a correct strategy to reduce the loss of unconsolidated material.

Finally an additional sealing test was performed. The Sample Vessel was filled with water, closed with the capping mechanism, weighed, and then placed into a Thermal Vacuum (TV) chamber; weighing it again, after some time spent in TV condition. Test conditions were selected for boiling water: 0.5 atm & 85 °C. The tests showed that the seal was not successful. The tests were too brief to be certain of the cause, but the use of a lead gasket instead of a gold one could be a factor.

2.4. Summary of sample packaging tests

All nominal tests have been successful, and the conceived handling system shown its capability to perform as planned. The mechanical interfaces have shown alignment capabilities even better than foreseen, in particular the SCM- SV cap interface, which was able to correct very large misalignments. SCM motors were properly sized, and performed without any problem.
Also, the sample extraction could be performed without any damage to the solid sample. The collection of loose samples has shown the need for some refinement, and a dedicated test program, of the sample vessel design and its' interface to the drill tool.

Although the BB was not conceived to evaluate the sealing performances of the SV design, a sealing test was valuable in demonstrating the criticality of the SV sealing. If a vessel with high sealing capability is required then a dedicated development and test campaign would be necessary

3. END-EFFECTOR

Following a critical evaluation at the preliminary design stage, one design was selected for detailed design followed by bread-boarding and testing. This was the bayonet-catch end-effector. Two similar designs (each had a generic screw-driver mechanism) - a three-finger design and an inner-jaw design- were slightly less favourable mainly because of extra complexity. Also, the Bayonet Catch design was selected over the inner-jaw end effector because of the maturity and high operational reliability of the traditional bayonet concept.

3.1. Design

A detailed view of the Bayonet-catch End-effector is shown in Figure 8, below. The key features of the Bayonet Catch end effector include:

- Spherical shaped nose – to aid alignment (+/- 5 mm, +/- 5°)
- Retractable hex-key for tightening
- Custom made interchange (Al or Ti) locking jaws – to assess robustness
- Partial labyrinth seals – for dust protection
- 2 stage harmonic drive – for high gear ratio
- Inner and outer Heaters (10 Watt each) – to increase operating temperature
- Maxon RE-30 motor – for tightening
- Maxon RE-13 – for locking
- Micro-switches – for accurate control and prevention of unintended release

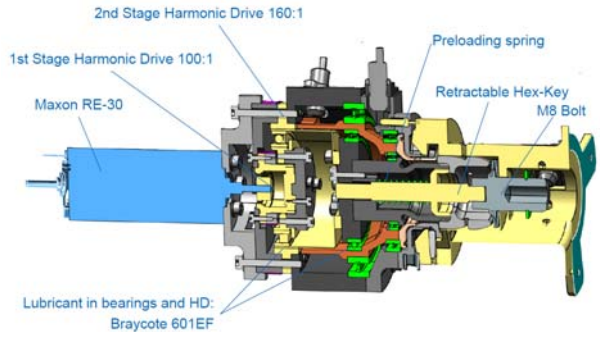

Figure 8- Section view of the End-Effector breadboard

This figure shows coloured functional parts, including the hex-key engagement with the Sample Container interface. The functionality of the End–Effector is designed to ensure that once the robotic arm has aligned the bayonet nose with the Sample Container I/F, the hex-key can retract under the mating forces to allow full engagement. The locking motor then activates the locking jaw blades, which rotate about the axis into the Sample Container interface void to lock the End-Effector to the interface.

Activating the tightening motor then rotates the preloaded hex key, to allow it to spring into the tightening bolt hex I/F. Once the hex key is engaged the tightening motor is then capable of applying ~40Nm of torque to tighten the Sample Container I/F bolt, this torque could be used to preload Sample Container halves together. The process can then be reversed to disengage the End-Effector and robotic arm from the Sample Container I/F.

Following a detailed design of the locking jaws and the screw-driver mechanisms, an end-effector breadboard was manufactured for testing (Figure 9). This breadboard was subjected to a comprehensive test campaign.

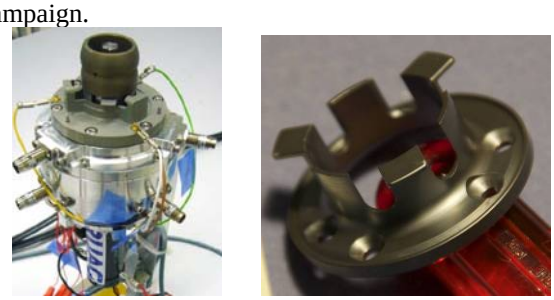

Figure 9 (a) End-effector Breadboard, (b) Locking Jaws Attachment

3.2. Test objectives

The Bayonet-catch End-effector was comprehensively tested at RUAG Space, with the following objectives. Prove the correct functioning of:

(a) the self-alignment feature.
(b) the gripping function (powered & unpowered state)
(c) the tightening/un-tightening (screwdriver) feature (under Mars conditions – dust, low temperature, mechanical loads, operational life, etc.).

For each of the above objectives, a dedicated test scenario was established and test performed.

In addition to such characterisations of functional performance, an overall aim was to verify that the breadboard (which was designed to be close to a flight model in terms of overall dimension, mass and functionality) was a feasible design that could lead to a flight model.

3.3. Test Results

A summary table of key results is shown in Table 1.

Table 1 End-effector test results

Test	Expected Result	Actual Result	Observations
Alignment:	Misalignment:	Misalignment - Force:	
Lateral	5 mm	6 mm – 2.4 N	Pass
Angular	5°	10° - 1.7 N	Pass
Orientation	5°	10° - 0.78 N	Pass
Lateral and Angular	5mm/5°	5mm/5° - 1.7 N	Pass
Angular and Orientation	5°/5°	5°/5° - 1.5 N	Pass
Lateral, Angular and Orientation	5 mm/5°/5°	5 mm/5°/5° - 1.9 N	Pass
Locking:	Max Motor Current:	Max Motor Current – Time:	
Locking	<0.5 A	0.11 A – 58.6 sec	Pass
Unlocking	<0.5 A	0.09 A – 59.3 sec	Pass
Tightening:	Max motor Current:	Max Motor Current – Time:	
Tightening	<4.0 A	0.676 A – 6 min 10 sec	Pass (1)
Un-tightening	<4.0 A	0.683 A – 7 min	Pass (1)
Torque Capacity:	40 Nm	> 40 Nm	Pass
Thermal Functional: +20°C/-55°C Locking & Tightening	Successful	Successful	Pass (2)
Thermal Tests:			
Heating -55°C to -20°C (worst case)	-	1 hr 51 min	- (3)
Heat Capacity:	-	2737 J/K	-
Dust Tests:	Force :	Force :	
Angular Misalignment	-	3.5 N	Pass
Lateral Misalignment	-	2.33 N	Pass
Orientation Misalignment	-	4.66 N	Pass (4)
Lateral+Angular Misalignment	-	2.44 N	Pass
Angular+Orientation Misalignment	-	3.5 N	Pass
Locking	Successful Locking	Successful	Pass (5)
Tightening	Successful Tightening	Successful	Pass
Separation	Successful Separation	Hex-Key Jammed	Fail (6)
Locking Cycling:	> 35 cycles	> 35 cycles achieved	Pass (7)

Notes:
(1) Tightening and un-tightening were successful; however some local deformation of the stainless steel hex key occurred.
(2) Locking and tightening were successful, however the locking time at -55 °C is 3.5 min longer than at ambient
(3) Two ten Watt heaters had to be used instead of the two 3 Watt heaters planned.
(4) Misalignments applied in dust conditions were as per the success criteria, the orientation alignment force (in axis) in dust was 530 % higher than without dust.
(5) Maximum locking currents in dust are significantly higher (~2-4 x) in dust than without, due to increased friction.
(6) After the functional test in dust it was not possible to remove the hex-key from the screw nut without disassembly - due to the cohesive dust grains filling the gaps and some local deformation of the uncoated stainless steel hex key.
(7) Al locking jaws were used for the dust test; Ti locking jaws were successfully used for the 35 cycle locking test.

3.4. Summary of end-effector test results

A bayonet-catch end-effector has been shown to be a robust design, able to self-align with a sample container, in the presence of significant lateral and angular misalignments. The grappling and locking design has been proven to operate reliably, including life-time locking tests and testing to -55C. No un-intended releases occurred.

Dust tests were particularly interesting – showing how the required motor currents were significantly increased for locking and tightening, but also showing some dust ingress into bearings and the hex key (used to secure the two sample container halves), leading to the jamming of the key at one point. These have led to recommendations for future work. I.e. redesign of the hex key and some redesign of the position/status sensors is desirable, including the electrical interface that avoids unintended release to make it more robust against dust.

4. ROBOTIC ARM CONTROL

The robotic arm control sub-system is a key element of the sample transfers. The critical operations of the SC-to-MAV transfer scenario (e.g. the approach, or the grasping) require accurate positioning of the end-effector referred to the grapple-fixture of the sample container. I.e. they require the use of vision-based control [3], and hybrid position-force/torque motion control for the SC extraction/insertion operations. Vision-based control is an enabling technology for robotic applications that require precise interactions with the environment. Vision processing of images allows the robot to 'know' the precise position of the grasping-fixture of the sample container. The alternative 'deterministic control' approach was considered inadequate for precise positioning of the robotic arm's end-effector when the position of the sample container on a rover is not precisely known.

Two different approaches are compared for vision-based control. The first is the 'look-and-move' approach, where the object to be approached is localised in the image and the robot is moved using only this information. Or, there is the 'Visual-servoing' approach, where visual features and then the robot control commands are computed for each new image acquired by the camera, until convergence is achieved.

4.1. Validation by simulation

The specified robotic activities and the associated control laws are simulated and analysed with respect to the positioning accuracy, the maximum tracking error in the controlled space (joint, Cartesian, sensor), the maximum generated forces during contact operations and the robustness referred to the initial conditions, calibration errors, visual targets design and environmental conditions.

The software simulation environment is an instantiation of the 3DROV tool [4] for planetary robotized systems design and simulation. The main elements of the simulator (as illustrated in Figure 10) are:

- The Physical sub-system block includes models of the physical sub-systems, motors and sensors. They are mainly modelled in the 20Sim engineering tool
- The Generic Controller assumes the role of the onboard flight software and controls the overall operations. It is modelled as a SIMSAT component.
- Environment component; provides the atmospheric conditions (dust, solar flux, temperatures, etc), and the ephemeris/timekeeping The Martian atmosphere is from the Mars Climate Database.
- The 3D Visualisation component is used to visualise in 3D the evolution of the simulation. This component is also used for images generation to feed the vision based control and force/torque generation used as input to the force/torque control.
- The Simulation Framework relies on ESA's SIMSAT tool and is responsible for the proper execution and scheduling of the simulation run.

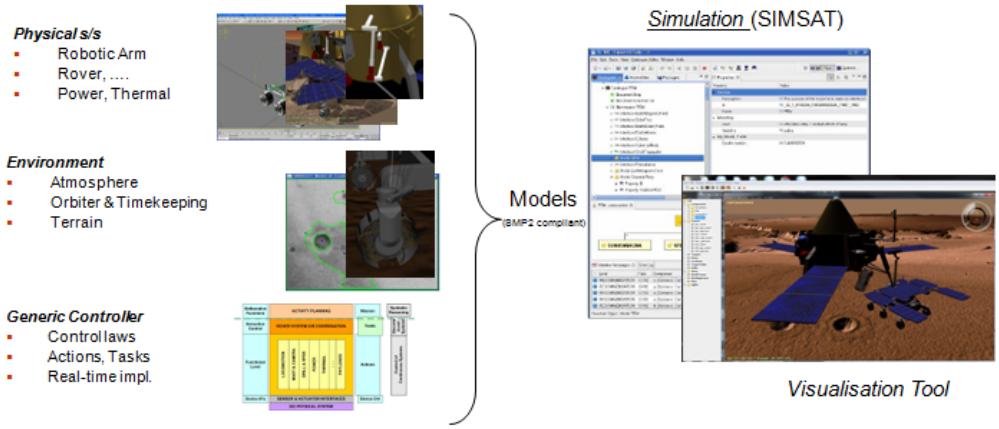

Figure 10 - Simulator Elements

4.2. Simulation Results

Free motion operations, in the joint and the Cartesian space, are simulated and the control laws are evaluated:

- to ensure the feasibility of the operations, in terms of the arm's ability to reach of all the positions it needs to visit.
- to evaluate the corresponding control laws in terms of accuracy and maximum tracking error,
- to evaluate the requested joint torques and finally to investigate the effects of the flexibility of the arm.

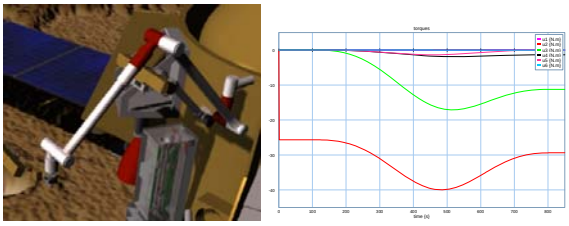

Figure 11 - Robotic arm simulation

The figure above illustrates the final robot positions of the 'move to standby' activity, and the associated maximum tracking error and the requested joint torques. The positioning accuracy of the control law is high with a very small maximum tracking error. The maximum torque is applied at the second joint (~40.0Nm).

When flexibility (of the arm limbs) is included in the model of the robotic arm a deviation of ~4mm is observed. This deviation has been checked to be compatible with the vision based control initialisation requirements.

Vision based control simulations are performed to characterise the visual targets, to identify the most appropriate configuration of the vision system and to evaluate, under different environmental conditions, the accuracy/repeatability/robustness of the visual servoing.

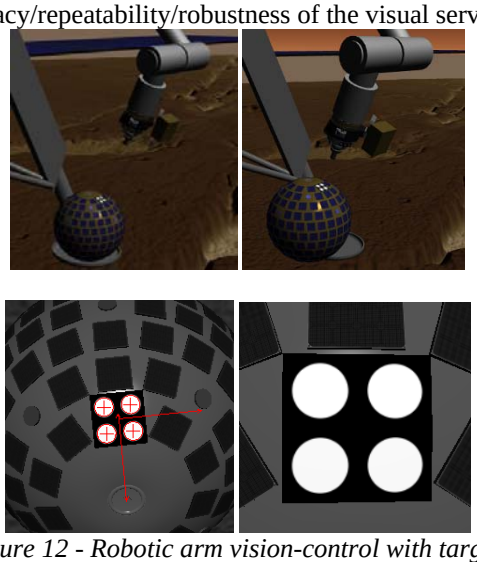

Figure 12 - Robotic arm vision-control with targets

The figure above illustrates the initial and the final robot positions and the corresponding target views during a simulation session. The results show that, the accuracy of the vision based control is high (at the order of 0.1mm). The repeatability also is very high showing the efficiency of this approach. The results remain excellent even when starting with a significant error in position/orientation, provided that the target remains in view of the camera.

Comparison between the visual servoing and the 'look and move' showed that the 'look-and-move' strategy provides a poor positioning accuracy Therefore, this strategy, under nominal environmental conditions, does not give adequate precision for grasping. Visual servoing tests, under various environmental conditions (over/under exposed images, presence of dust, etc), have given information on the limits of the tracking process.

The hybrid position - force torque control used during the 'attach' phase of the SC transfer operations are also simulated. The attach sequence is executed several times under different initial positions covering a range of 20mm and 4.0deg referred to the optimal positioning of the EE in front of the grapple-fixture of the sample container. At contact, the normal force is measured at 15N and remains at 1N when sliding on the one side of the SC surface. During insertion, the force is regulated to 0N while position control is performed at the insertion direction.

4.3. Hardware-based testing of Vision Control

Vision based control is also validated by experiments with real hardware using the following set-up:

- the Eurobot Ground Prototype (see Figure 13) and it's controller
- A camera Marlin F-80C attached on the EE of the target robotic arm and a PC controller.
- A set of spot lights positioned on the robotic system to provide different illumination conditions.

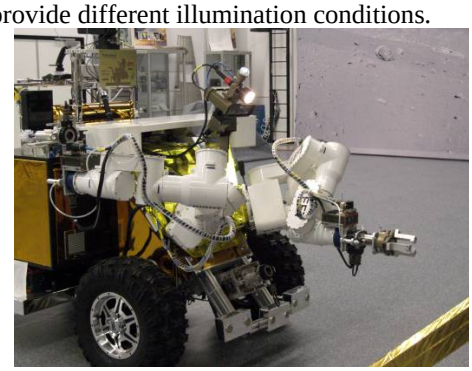

Figure 13 -Eurobot test setup for vision control tests

The accuracy and the repeatability of the visual servoing have been evaluated considering different initial positions of the camera with respect to the target. The figure below illustrates the initial robot position and the corresponding target view. The results are based on the use of a 4-dot target, which is well known for its simplicity and robustness.

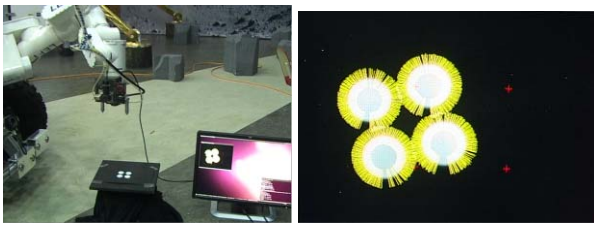

Figure 14 - Robotic arm vision tests with target images

The accuracy of the positioning for each direction is evaluated at:

- Tx= 0.095mm, Ty= 0.145mm, Tz= 0.33mm
- Rx = 0.1mrad, Ry = 0.17mrad, Rz = 0.19 mrad.

Visual servoing has been tested with occluded targets (up to ~30% of one of the dots) and in presence of moving shadows.

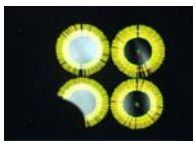

Figure 15 - Occluded targets for vision tests

The robustness of the tracking algorithm is very high since, despite significant occlusion and shadows, the positioning accuracy and repeatability are excellent providing equivalent results to those reported above.

From the experimental results we can draw the following conclusions:

- Visual Servoing using the eye-in-hand configuration (the camera attached on the EE) can be applied with a very poor camera calibration.
- The accuracy of the positioning tasks has been identified to be at sub-millimetre level
- The repeatability of the positioning task using Visual Servoing is excellent (~0.01mm Std. .dev.).
- The tracking aspects constitute a major contribution of these experiments. In particular, the 'Moving Edges' algorithm has tested and shown to be robust in presence of changing environmental conditions and targets occlusion.
- Executing the same algorithms and code as the ones used for the simulations, has given confidence in the simulations by giving comparable results on accuracy and repeatability.

5. CONCLUSION

The breadboard tests have demonstrated the general feasibility of the sub-systems that have been designed.

The sample packaging (capping/uncapping mechanism, sample vessel design and sample container positioning to collect samples from a drill) was successfully tested. The tests led to recommendations for further refinement, particularly associated with the sample vessel design.

Similarly the bayonet-catch end-effector was extensively tested and was successfully operated, including thermal and life-cycle tests. Recommendations have been made for further work, especially for improvements of the tightening hex-key.

Extended simulations of the transfer of a sample container have allowed us to simulate and tune the robotic-arm control, including power/energy use). Accurate/repeatable sub-mm positioning has been demonstrated - with vision-based closed-loop control. Hardware tests have given confidence in the simulations, by giving comparable results on accuracy and repeatability.

This study has investigated the key functionalities of the end-end robotic chain for sample handling and provided a valuable insight into the design of such sample transfer systems for the MSR programme. The prototyping and testing of the selected critical elements of this chain has further enhanced our understanding of the operation and limits of such systems beyond the direct application to MSR of any sample handling

6. ACKNOWLEDGEMENTS

The authors acknowledge the support of the European Space Agency, which funded the MSSTM study on which this paper is based.

The author list shows the international team that worked on this study. Also, EPFL (Reto Wiesendanger) provided valuable support for the end-effector concepts and preliminary design, with Beat Zahnd (Ruag), and with additional contributions from Oxford Technologies Ltd, UK. Piergiovanni Magnani contributed to the Selex-Galileo work on sample packaging. Mark Sims and John Bridges, University of Leicester UK, and Dave Barnes, Aberystwyth University UK, provided consultancy support – particularly on science issues relating to sample handling and on robotics simulations, respectively.

7. REFERENCES

1. Allouis, E, et al (2010). End-to-end Design of a Robotic System for Collecting and Transferring Samples on Mars, *proc. i-SAIRAS conference, Sapporo, Japan, Aug 2010*.

2] Magnani P. et al (2010). Exomars Drill for Subsurface Sampling and Down-Hole Science, IAC conference, Prague, Czech Republic, Sept 2010.

.3. K. Kapellos, F. Chaumette , M. Vergauwen, A. Rusconi, L. Joudrier: "Vision Based Control for Space Applications", iSAIRAS 2008.

4. K. Kapellos, L. Joudrier: 3DROV - A Planetary Robotic System Design Tool Based on SimSatV4, ESAW 2009.